Korean J. Chem. Eng., 38(4), 756-762 (2021)
DOI: 10.1007/s11814-020-0738-4

pISSN: 0256-1115
eISSN: 1975-7220

Effects of chloride and other anions on electrochemical chlorine evolution over self-doped TiO_2 nanotube array

Teayoung Lee*, Seongsoo Kim*, Joon Young Choi, Changha Lee*, Choonsoo Kim***,†, and Jeyong Yoon*,****,†**

*School of Chemical and Biological Engineering, Institute of Chemical Processes (ICP), Seoul National University, 1 Gwanak-ro, Gwanak-gu, Seoul 08826, Korea
**Hyorim Industries Inc., 96-8, Yatab-ro, Bundang-gu, Seongnam-si, Gyeonggi-do 13517, Korea
***Department of Environmental Engineering and Institute of Energy/Environment Convergence Technologies, Kongju National University, 1223-24, Cheonan-daero, Cheonan-si 31080, Korea
****Korea Environment Institute, 370 Sicheong-daero, Sejong-si 30147, Korea
(*Received 25 October 2020 • Revised 21 December 2020 • Accepted 23 December 2020*)

Abstract−Electrochemically reduced TiO_2 nanotube arrays (r-TiO_2 NTA) have emerged as an alternative that can replace the dimensionally stable anode (DSA®) due to comparable performance for chlorine evolution reaction (ClER). However, previous studies have reported applications of r-TiO_2 NTA for ClER only under limited conditions (concentrated NaCl solution without other anions). Thus, the potential of r-TiO_2 NTA for CIER has not yet been fully demonstrated. Therefore, this study focused on investigating ClER of r-TiO_2 NTA under various parameters such chloride concentration (5-1,000 mM) and the presence of other anions (i.e., SO_4^{2-}, HPO_4^{2-}, and CO_3^{2-}). The results suggest that, at low chloride concentration (5-50 mM NaCl), the r-TiO_2 NTA exhibited higher performance for CIER (production rate of 3.35-9.82 mg l^{-1} min^{-1}, current efficiency of 14.43-42.04%, energy consumption of 69.24-11.02 Wh $g(Cl_2)^{-1}$) than RuO_2 (2.55-7.88 mg l^{-1} min^{-1}, 11.07-33.85% and 77.29-6.84 Wh $g(Cl_2)^{-1}$, respectively). Additionally, other anions did not affect the ClER of r-TiO_2 NTA more than RuO_2. These can be explained by the indirect pathway of ClER in r-TiO_2 NTA while the direct pathway of RuO_2 was negatively affected by dilute chloride and other anions.

Keywords: Reduced TiO_2 Nanotube Array, Electrochemical Self-doping, Chlorine Evolution, Chloride Concentration, Anion Effect, Hydroxyl Radical

INTRODUCTION

The electrochemical oxidation process (EOP) has been extensively studied in the water treatment field due to its various advantages such as ease of operation, lack of requirement of additional chemicals, and high effectiveness for the production of various oxidants during the electrolysis of water [1,2]. Chlorine is a well-known fundamental oxidant produced by EOP that has been utilized for the degradation of organic pollutants and disinfection of water [3-5]. Several operational parameters such as electrode materials, operational modes regarding the application of current and voltage, and feed conditions (i.e., pH, composition and temperature) govern the efficiency of oxidant production via EOP [6]. Among them, anode materials are primarily responsible for the production of oxidants in high yield [3]. The dimensionally stable anode (DSA®) is a commercially available anode that has been widely used for the effective production of chlorine [7-9].

TiO_2 nanotube array (TiO_2 NTA) has garnered considerable attention as a promising anode material for EOP because it has numerous beneficial properties such as highly aligned open pore nanostructure, large surface area, and chemical stability [10,11]. In addition, it can be easily fabricated via electrochemical anodization, and a well-organized nanostructure can be established onto a titanium substrate without requiring additional processes for TiO_2 [12-14]. The facile fabrication of the TiO_2 NTA allows them to be employed for various applications. Despite these advantages, they have been limited to applications as an anode material for oxidant production because they are semi-conductive and thus exhibit low electrocatalytic activity [15]. To overcome this, various approaches such as thermal hydrogenation and incorporation of metal and non-metal impurities have been proposed [16-20].

Electrochemical self-doping is another method to enhance the electrocatalytic activity of the TiO_2 NTA. This process involves forming reduced TiO_2 NTA (r-TiO_2 NTA) by electrochemical reduction possibly leading to trivalent titanium as self-dopant. The electrochemical reduction of anatase TiO_2 NTA (a-TiO_2 NTA) converts the surface a-TiO_2 NTA from gray to blue. It is attributed to the significantly improved dopant level of r-TiO_2 NTA via electrochemical reduction compared to a-TiO_2 NTA [21]. Unlike the process of impurity incorporation, the electrochemical self-doping process imparts high structural stability to the TiO_2 NTA because of the formation of Ti^{3+} that causes a small distortion in the crystal structure and surface morphology of the TiO_2 NTA [22]. After doping, the r-TiO_2 NTAs exhibited significantly improved capacitive and

†To whom correspondence should be addressed.
E-mail: choonsoo@kongju.ac.kr, jeyong@snu.ac.kr

electrocatalytic activity for the chlorine evolution reaction (ClER); their performance was comparable to that of the commercially available DSA® [23-26]. Therefore, there have been many studies with r-TiO_2 NTA for environmental applications (e.g., energy storage device, wastewater treatment, disinfection and desalination) [27-31].

However, the chlorine evolution performance on r-TiO_2 NTA has been demonstrated in limited experimental conditions with highly concentrated NaCl solution (i.e., high concentration of chloride (Cl^-) ions as a precursor for electro-generated chlorine (Cl_2), $2Cl^- \rightarrow Cl_2+2e^-$, E_0=1.36 V vs NHE). Thus, the r-TiO_2 NTA was not utilized in practical environmental and industrial applications. Consequently, in order to expand its application spectrum, the performance of the ClER over the r-TiO_2 NTA at low Cl^- concentration and in the presence of other anions needs to be investigated. This will facilitate the application of the TiO_2 NTA for the treatment of tap water, ground water, and wastewater. Therefore, it is necessary to assess the features of the ClER over r-TiO_2 NTA under various conditions to verify their applicability as an anode for EOP.

In this study, we attempted to verify the potential of r-TiO_2 NTA for the ClER at various Cl^- concentrations ranging from 5 to 1,000 mM and in presence of other anions (e.g., SO_4^{2-}, HPO_4^{2-}, and CO_3^{2-}). The electrocatalytic property of r-TiO_2 NTA was compared to that of RuO_2, which was one of the representatives for DSA®. In addition, the advantages of r-TiO_2 NTA for ClER in the conditions were elucidated by revealing its indirect mechanism for ClER with *t*-BuOH.

EXPERIMENTAL SECTION

1. Fabrication of Electrodes

The r-TIO_2 NTA was synthesized via the electrochemical self-doping of the anodized TiO_2 NTAs (anatase) by following previously reported procedures [23-26]. In brief, the TiO_2 NTA were prepared by anodization in 30 mL electrolyte containing H_2O (2.5 wt%), NH_4F (0.2 wt%), and ethylene glycol (97.3 wt%) at a constant voltage of 40 V for 5 h. Titanium foil (1 cm×2 cm) and platinum mesh were selected as the anode and cathode, respectively. The synthesized TiO_2 NTA were completely purified using deionized water (DI), followed by a thermal treatment at 450 °C for 1 h under atmospheric conditions. The electrochemical self-doping of the thermally treated TiO_2 NTA (anatase; a-TiO_2 NTA) was performed in a phosphate buffer solution (PBS; 0.1 M KH_2PO_4 with NaOH, pH 7.2) and −16.7 mA cm^{-2} for 90 sec. The RuO_2 electrocatalyst was prepared by dropping 50 μl of the ruthenium precursor ($RuCl_3 \cdot H_2O$ 0.2 M (HCl : DI=1 : 1) on a titanium plate that was treated with 1 M HCl at 80 °C for 30 min, followed by annealing at 450 °C for 1 h.

2. Surface and Electrochemical Properties

The morphology of the r-TiO_2 NTAs was examined by scanning electron microscopy (SEM; JSM-6700F, JEOL, Japan). X-ray diffraction (XRD) analysis (Bruker D8 DISCOVER, Germany) was conducted to characterize the material of r-TiO_2 NTA. The electrochemical property of the r-TiO_2 NTAs was investigated through staircase linear sweep voltammetry (SLSV) (PARSTAT 2273A, Princeton Applied Research, U.S.A.).

The level of dopant (charge carrier density) of a-TiO_2 and r-TiO_2 NTA was estimated with Mott-Schottky plot (Eq. (1)), which was obtained via EIS measurements of the complex capacitance at AC potential of 10 mV and DC potential of open circuit potential in 0.1 M phosphate buffer solution (PBS).

$$\frac{1}{C_{sc}^2} = \left(\frac{2}{e\varepsilon_0\varepsilon N_D}\right)\left(E_{app} - E_{fb} - \frac{kT}{e}\right) \quad (1)$$

where C_{sc}^{-2} is the space charge capacitance ($F^{-2} \cdot cm^4$), E_{app} and E_{fb} indicate an applied potential and flat band potential, respectively. N_D is the donor density (cm^{-3}) and e is the electronic charge. ε is the dielectric constant of TiO_2 ($\varepsilon(TiO_2)$=31 for anatase, Ref. of [20]) and ε_0 is the permittivity of the free space. k is the Boltzmann constant and T is the operational temperature.

To understand the ClER on r-TiO_2 NTA, the ohmic drop was corrected with Eq. (2) and (3) as below [25,32].

$$\frac{\Delta\eta}{\Delta i} = \frac{b}{i} + R \quad (2)$$

$$\eta_{corr} = \eta - iR \quad (3)$$

where η, i, b, and R represent the overpotential, current in the SLSV, Tafel slope (V dec^{-1}), and total area of uncompensated resistance (Ω cm^2), respectively.

3. Evolution of Chlorine and other Oxidants

Cl_2 was electrochemically produced in an undivided electrocatalytic cell (30 ml) with various NaCl concentration ranging from 5 to 1,000 mM in the absence and the presence of sodium salts of the following anions: HPO_4^{2-}, SO_4^{2-}, and CO_3^{2-} (Sigma Aldrich Co.). The Cl_2 and other oxidant concentration (mg l^{-1} as total Cl_2) was quantitatively measured by the *N*,*N*-diethyl-*p*-phenylenediamine (DPD) colorimetric method using a spectrophotometer (DR/900, HACH Co., Loveland, USA) at 530 nm [3]. To examine the effect of anions, each anion was electrolyzed in the absence of Cl^- and the capability of generated oxidants was measured with the same DPD which has potassium iodide (KI). The ionic strength of the electrolyte was maintained by using $NaClO_4$ as a supporter solution in the same amount as the 1,000 mM NaCl solution.

The mechanism of ClER over the TiO_2 NTAs and RuO_2 was elucidated by following the terephthalic acid (TA; 0.1 mM) degradation on each electrode using high-performance liquid chromatography (HPLC; YL9100, Younglin Co., Korea) performed in a methanol and formic acid (0.1%) mixture (v/v, 60 : 40) [33]. The effect of hydroxyl radicals (·OH) on the ClER was examined by adding 0.03-1 M *t*-BuOH and by conducting a scavenging test during chlorine production [23].

The current efficiency and energy consumption for generation chlorine were calculated by Eqs. (4) and (5), respectively.

$$\text{Current efficiency (\%)} = \frac{nFCV}{itM_{Cl_2}} \quad (4)$$

$$\text{Energy consumption } (Wh \cdot g^{-1}) = \frac{i\int edt}{CV} \quad (5)$$

where C is the concentration of electro-generated chlorine (g l^{-1}), V is the volume of electrolyte (l), n is the number of electrons (1

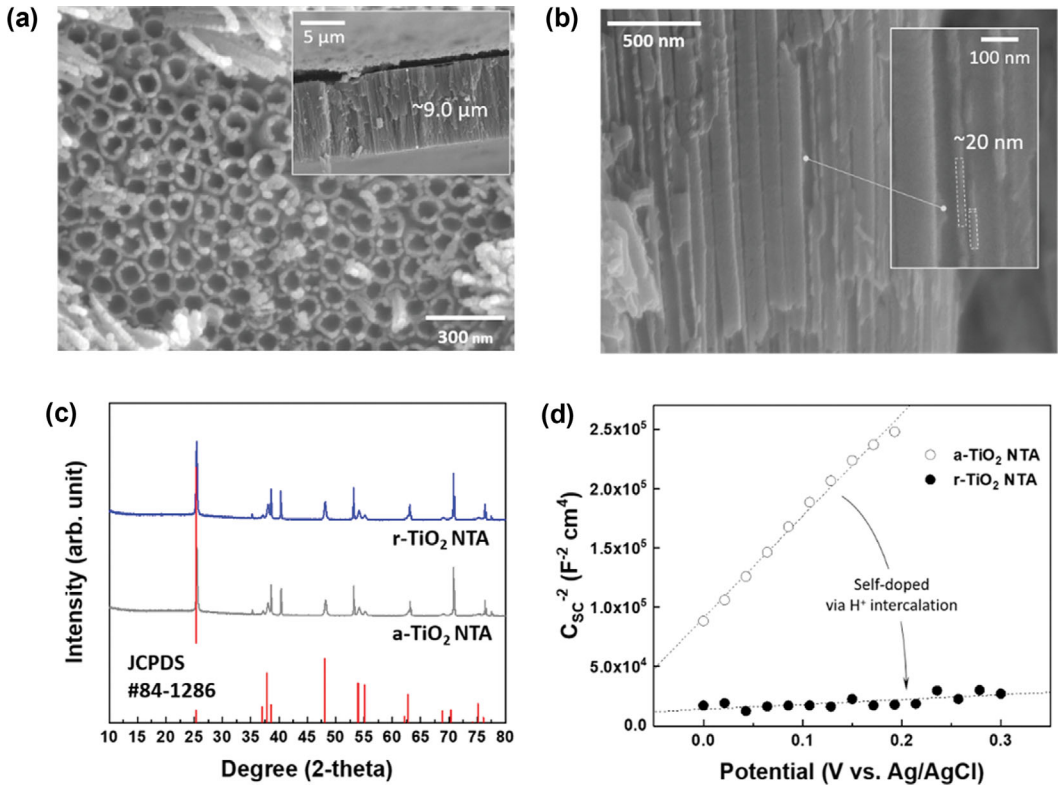

Fig. 1. Surface morphology and characteristics of the reduced TiO_2 nanotube array (r-TiO_2 NTA): (a) top and (b) cross-sectional views of the scanning electron microscopies (SEM), (c) X-ray diffraction (XRD) patterns, and (d) Mott-Schottky plot of r-TiO_2 NTA; The inset of panel A indicates the thickness of r-TiO_2 NTA and the XRD patterns of the anatase TiO_2 NTA (a-TiO_2 NTA) were indexed with reference to the JCPDS file (PDF 84-1286). The Mott-Schottky plot was obtained with AC potential of 10 mV (frequency=100 Hz) and DC potential of open circuit potential in 0.1 M KH_2PO_4 with NaOH (pH of 7.2).

eq mol^{-1}), F is the Faradaic constant (96,485 C eq^{-1}), M_{Cl_2} is the molecular weight of chlorine (71 g mol^{-1}), i is applied current (A) and t is the electrolysis time (s), and e is the operational cell voltage (V).

RESULTS AND DISCUSSION

Fig. 1 shows the surface morphology and doping level of the prepared r-TiO_2 NTA as examined by the SEM images ((a) and (b)), XRD patterns (c), and Mott-Schottky plots (d) of the sample. As shown in Fig. 1(a) and (b), the r-TiO_2 NTA have a well-organized nanostructure with a pore size, wall thickness, and tube length of approximately 111.5 (±16.6) nm, 20 nm, and 9.0 μm, respectively. The XRD pattern (Fig. 1(c)) shows that the peak positions of the r-TiO_2 NTAs are consistent with those of the a-TiO_2 NTA (JCPDS, PDF 84-1286), implying that electrochemical self-doping has a negligible effect on the structural property of the r-TiO_2 NTA. However, a significant improvement in the doping level was observed in the r-TiO_2 NTA (Fig. 1(d)). The slope of the Mott-Schottky plot for the r-TiO_2 NTA was much smaller than that of the pristine a-TiO_2 NTA, indicating a high doping level of the r-TiO_2 NTA. These findings are in accordance with previous studies [21], and accordingly we can confirm that the r-TiO_2 NTA was well synthesized.

The electrocatalytic activity of the r-TiO_2 NTAs and RuO_2 for the ClER was examined by investigating the concentration (mg l^{-1}) of electro-generated chlorine, its production rate (mg l^{-1} min^{-1}), charge efficiency (%), and energy consumption (Wh g^{-1}). The results of the analyses are presented in Fig. 2. Fig. 2(a) shows a linear correlation between the chlorine produced over the r-TiO_2 NTA and RuO_2 and the electrolysis time at various Cl^- concentrations. Clearly, increasing the NaCl concentration improved the production of Cl_2 in all samples. However, the r-TiO_2 NTA and RuO_2 displayed different chlorine evolution rates at different NaCl concentration (Fig. 2(b)). At low Cl^- concentration (5-50 mM NaCl), the r-TiO_2 NTA exhibit higher production efficiency with a Cl_2 generation rate of 3.35-9.82 mg l^{-1} min^{-1}, current efficiency of 14.43-42.04%, and energy consumption of 69.24-11.02 Wh $g(Cl_2)^{-1}$ than RuO_2 did (generation rate of 2.55-7.88 mg l^{-1} min^{-1}, current efficiency of 11.07-33.85%, and energy consumption of 77.29-6.84 Wh $g(Cl_2)^{-1}$). In contrast, at higher Cl^- concentration (100-1,000 mM NaCl), RuO_2 shows higher performance for the ClER. In particular, at 1,000 mM NaCl, the current efficiency of RuO_2 (~76%) is considerably higher than that of the r-TiO_2 NTA (64.83%). Thus, at low NaCl concentrations the ClER is favored over the r-TiO_2 NTA, whereas at higher concentrations it is favored over RuO_2. These results can be explained by the different mechanisms of the ClER on the r-TiO_2 NTA and RuO_2. To better understand the mechanism, the formation of ·OH was examined.

As shown in Fig. 3, the effect of ·OH on the ClER over the r-TiO_2

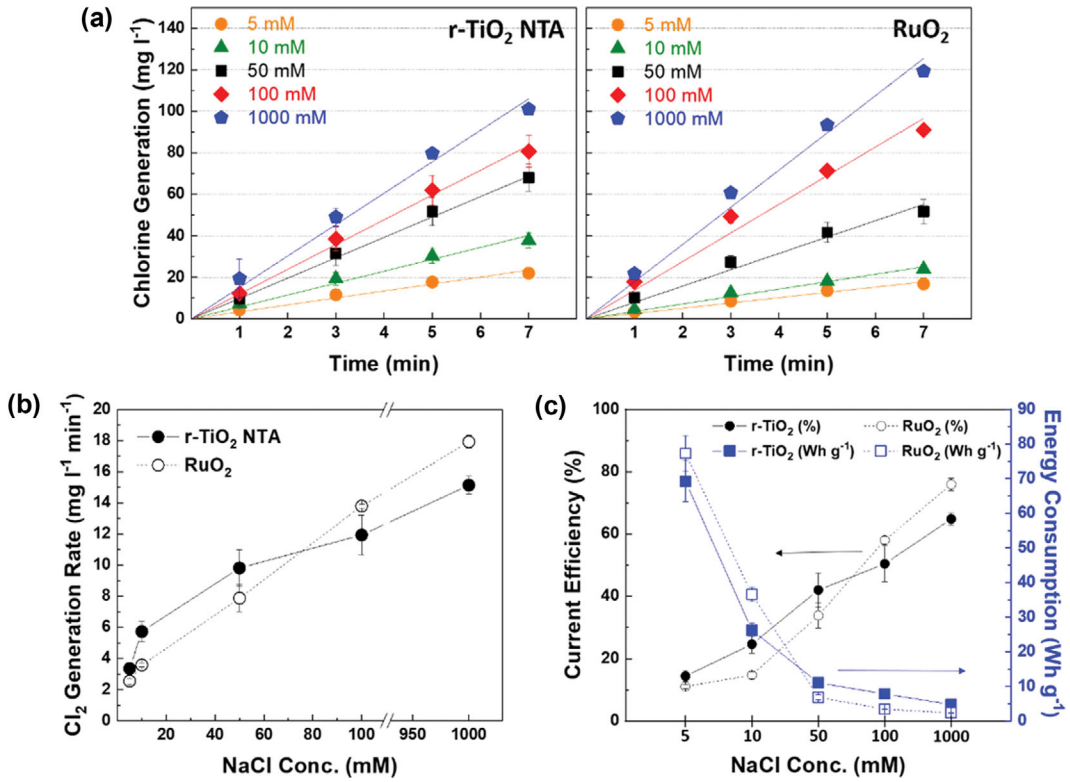

Fig. 2. Chlorine (Cl_2) evolution performance on r-TiO_2 NTA and RuO_2: (a) Cl_2 concentration, (b) Cl_2 evolution rate, and (c) current efficiency and energy consumption. The Cl_2 evolution was examined at a constant current of 16.7 mA cm^{-2} for various NaCl concentrations ranging from 5, 10, 50, 100, and 1,000 mM.

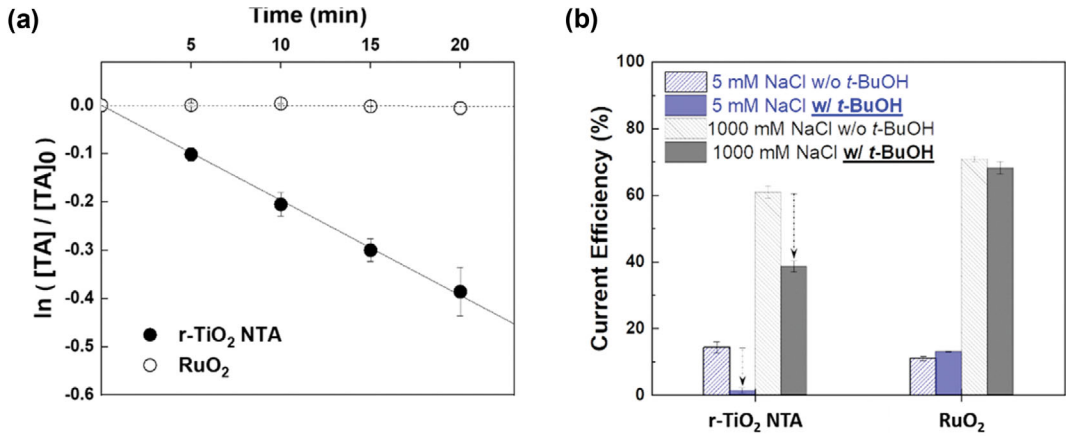

Fig. 3. (a) Production of hydroxyl radical examined by semi-log plot with 0.1 mM terephthalic acid solution as a hydroxyl radical (·OH) probe compound and (b) the effect of ·OH scavenger on chlorine (Cl_2) evolution (current efficiency) of reduced TiO_2 nanotube (r-TiO_2 NTA) and RuO_2: in panel A, the ·OH production was conducted in 0.1 M KH_2PO_4 with NaOH (pH of 7.2) under constant current of 16.7 mA cm^{-2} for 20 min. In panel B, the current efficiencies in 5 mM and 1,000 mM NaCl with addition of 0.03-1 M *t*-BuOH under applying constant current of 16.7 mA cm^{-2} for 5 min were presented.

NTAs and RuO_2 was investigated by examining the steady-state production rate of ·OH, which was determined by the degradation of an ·OH probe compound (terephthalic acid, 0.1 mM) and the ClER in presence of an excess ·OH scavenger (*t*-BuOH of 0.03-1 M). The ·OH production over the r-TiO_2 NTAs follows pseudo-first-order kinetics (linear slope in semi-log plot in Fig. 3(a)) [33] and the steady-state rate (~3.28×10^{-4} s^{-1}) is almost 200-times higher than that of RuO_2 (1.67×10^{-6} s^{-1}), indicating the high activity of the r-TiO_2 NTAs for ·OH production. The different behavior for ·OH production indicates that r-TiO_2 NTA and RuO_2 have the different ClER mechanism. In addition, the addition of excess *t*-BuOH, an ·OH scavenger, causes the ClER over the r-TiO_2 NTA to be completely inhibited in 5 mM and 1,000 mM NaCl; however, the ClER over RuO_2 remains largely unaffected (Fig. 3(b)). These findings

suggest that the ClER over the r-TiO_2 NTA is mediated by ·OH indirectly, but that over RuO_2 takes place via the direct oxidation of Cl^- ions on the surface [3]. In this regard, in dilute Cl^- solutions, wherein the mass transfer of Cl^- is limited, ·OH produced over the r-TiO_2 NTAs could oxidize Cl^- ions to Cl_2 via diffusion from the anode surface easier than RuO_2. In contrast, in highly concentrated Cl^- solutions, the mass transfer limitation of Cl^- is negligible; thus, RuO_2 which has the direct pathway for Cl_2 generation is more efficient in ClER than the r-TiO_2 NTA.

The role of ·OH in the ClER on r-TiO_2 NTA and RuO_2 is more clearly demonstrated by the current-overpotential curves measured using the SLSV method (Fig. 4). Note that the curves were adjusted by iR drop compensation to clarify CIER in various Cl^- concentration. As shown in Fig. 4, there are two major aspects on CIER of r-TiO_2 NTA and RuO_2. First, small differences in the SLSV curve on r-TiO_2 NTA were found at different Cl^- concentration during which RuO_2 exhibited a large dependency with Cl^- concentration. This implies that Cl^- concentration is a major factor to govern CIER on RuO_2 with direct oxidation. However, the effect of Cl^- concentration on ClER of r-TiO_2 NTA is negligible with the reaction pathway mediated by ·OH. Second, at low Cl^- concentration, although the current on r-TiO_2 NTA in SLSV is much less than that of RuO_2, r-TiO_2 NTA led to better CIER performance (Fig. 2) than RuO_2. It can be explained by that the indirect man-

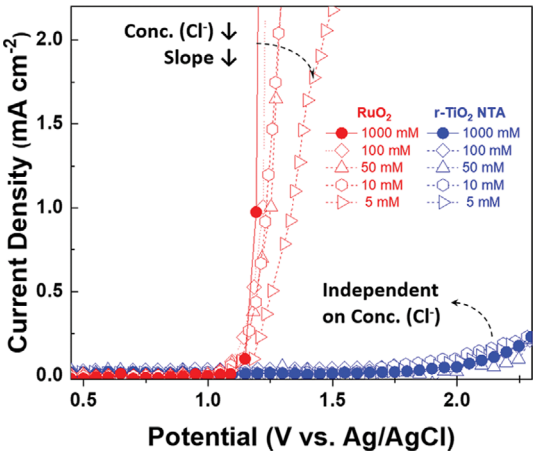

Fig. 4. Current-overpotential curves examined by staircase linear sweep voltammetry (SLSV) measurement of reduced TiO_2 nanotube array (r-TiO_2 NTA) and RuO_2 at various NaCl concentration ranging from 5 mM, 10 mM, 50 mM, 100 mM and 1,000 mM with a step height and step of 1 min (scan rate of 0.83 mV/s).

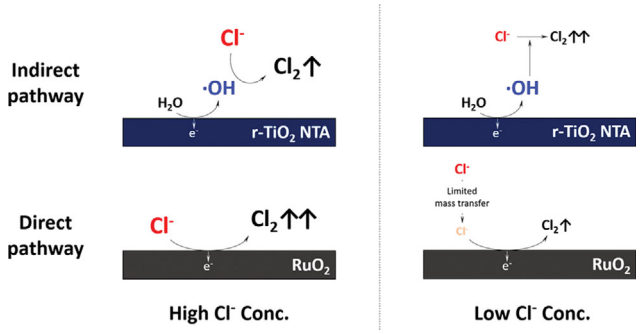

Fig. 5. Schematic illustration for the chlorine evolution mechanisms of r-TiO_2 NTA and RuO_2 in high and low chloride concentrations.

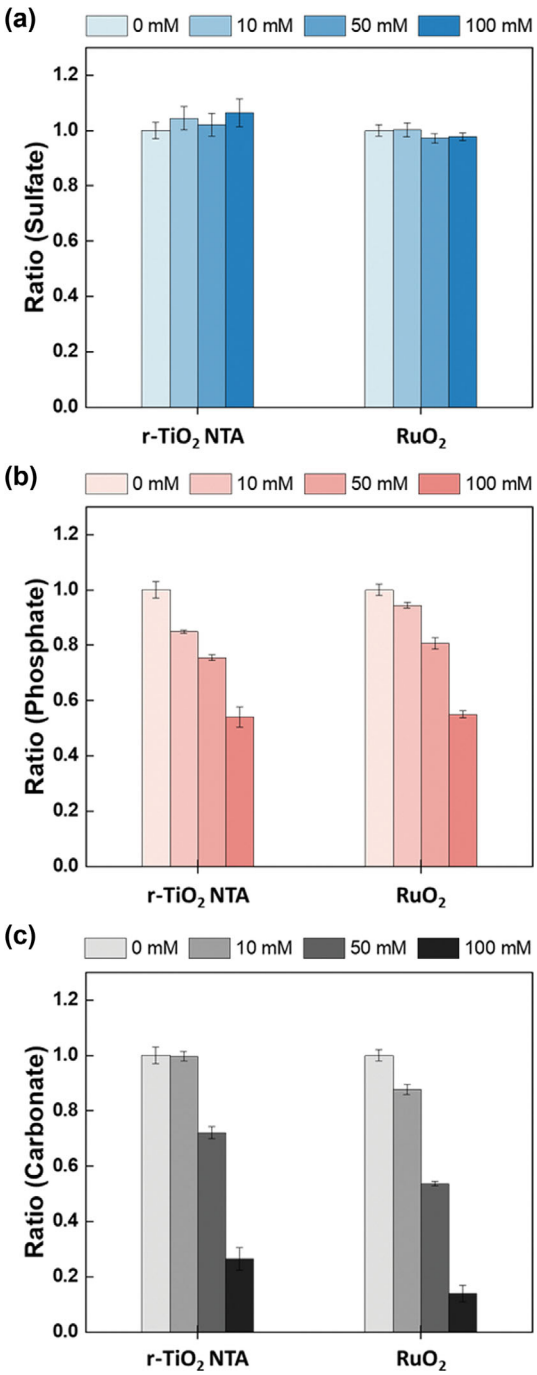

Fig. 6. Effects of anions including (a) SO_4^{2-}, (b) HPO_4^{2-} and (c) CO_3^{2-} on chlorine (Cl_2) evolution of reduced TiO_2 nanotube array (r-TiO_2 NTA) and RuO_2. Each generated Cl_2 in various anions was presented as a ratio to the result in the absent of the anions. Cl_2 evolution was conducted with a constant current of 16.7 mA/cm^{-2} at 1,000 mM NaCl with concentration of anions ranging from 10 to 100 mM for 7 min.

Table 1. Effects of anions for oxidant (Cl_2) formation in the presence and absence of chloride ion; DPD method, applied current density of 16.7 mA cm^{-2}, electrolysis time of 7 min, concentration of anions including HPO_4^{2-}, SO_4^{2-} and CO_3^{2-} of 50 mM in 1,000 mM $NaClO_4$ supporter electrolyte. Note that the results in the only Cl^- (1,000 mM) condition were from Fig. 2(a)

Unit: mg l^{-1} as Cl_2		Cl^- (Only)	SO_4^{2-}	HPO_4^{2-}	CO_3^{2-}	Supporter (ClO_4^-)
r-TiO_2 NTA	w/Cl^-	99.33 (±2.89)	101.33 (±4.04)	75.00 (±1.00)	71.67 (±2.08)	-
	w/o Cl^-	-	2.25 (±0.08)	0.59 (±0.01)	0.15 (±0.01)	0.04 (±0.00)
RuO_2	w/Cl^-	119.33 (±2.51)	116.00 (±2.00)	96.33 (±2.52)	64.00 (±1.00)	-
	w/o Cl^-	-	0.04 (±0.02)	0.03 (±0.01)	0.08 (±0.02)	0.02 (±0.001)

ner of r-TiO_2 NTA in ClER can lead to small effect of mass transfer of Cl^- via the diffusion of produced hydroxyl radical from the electrode surface at low Cl^- concentration. On the other hand, at high Cl^- concentration, small mass transfer limitation of Cl^- provide an optimized environment for ClER on both of the electrodes, and thus they can reveal the high ClER performance (refer to Fig. 5).

To further investigate chlorine evolution over the r-TiO_2 NTA, the effect of sulfate (SO_4^{2-}), phosphate (HPO_4^{2-}), and carbonate (CO_3^{2-}) ions on the ClER was examined (Fig. 6). As shown in Fig. 6, the presence of anions caused the ClER over the r-TiO_2 NTA and RuO_2 to be suppressed, and the extent of ClER suppression increased with the anion concentration. The addition of SO_4^{2-}, HPO_4^{2-}, and CO_3^{2-} ions caused the performance of ClER over RuO_2 to decrease: the production rate (~2.28 mg l^{-1} min^{-1}) and charge efficiency decreased by ~14% and 9.69%, respectively (Fig. S1 and S2), compared to those obtained in the absence of anions (Fig. 2). However, the effect of anions on the ClER over the r-TiO_2 NTA was relatively less significant than that over RuO_2. Exceptionally, the ClER of r-TiO_2 NTA was improved in the presence of SO_4^{2-}. Considering that the ClER of the r-TiO_2 NTA is mediated by ·OH (Fig. 3 and the detailed mechanism provided in previous studies [23,24,28]), it is plausible that reaction of ·OH and Cl^- ions is interfered in the presence of anions.

This can be well supported by the produced oxidants (Table 1). From the results in Table 1, the production of unspecified oxidants from the anions was confirmed by electrolysis with r-TiO_2 NTA in each anion, not including Cl^- ions. It is assumed that $P_2O_8^{4-}$, $S_2O_8^{2-}$, and $C_2O_6^{2-}$ were formed by the reaction between ·OH and the anions [31,34]. The oxidants formed on r-TiO_2 NTA were considerably higher than RuO_2. Interestingly, the presence of SO_4^{2-} resulted in higher yield of oxidants (~2.25 mg l^{-1} as Cl_2) compared to the HPO_4^{2-} and CO_3^{2-} (~0.59 mg l^{-1} as Cl_2 and ~0.15 mg l^{-1} as Cl_2, respectively). This indicates that SO_4^{2-} is more favorable for the reaction of ·OH, which can be a cause for the enhanced ClER of the r-TiO_2 NTA in the presence of SO_4^{2-}.

CONCLUSION

We evaluated the chlorine evolution on r-TiO_2 NTA under various experimental conditions including different NaCl concentrations and presence of interfering anions. The mechanism of ClER on the r-TiO_2 NTA was verified with a scavenging test of ·OH. As major results, first, r-TiO_2 NTA revealed better Cl_2 evolution performance than RuO_2 at low NaCl concentration ranging from 5-100 mM, while highly improved ClER performance on RuO_2 was found at high NaCl concentration (1,000 mM) compared to r-TiO_2 NTA. Second, in the presence of anions (i.e., SO_4^{2-} , HPO_4^{2-} and CO_3^{2-}), the ClER of r-TiO_2 NTA was slightly less suppressed than RuO_2. Considering the ClER mechanism of r-TiO_2 NTA mediated by ·OH, it is attributed to that the additional oxidants formed by the reaction of anions with ·OH leading to increase oxidant efficacy of CIER. This suggests the ·OH plays an important role in ClER of r-TiO_2 NTA. These results can provide a better understating the properties of r-TiO_2 NTA as an anode for ClER and open various opportunities for implantation of r-TiO_2 NTA in environmental and industrial applications. Additionally, with these results, it would lead to the further success of r-TiO_2 NTA to improve the stability of r-TiO_2 NTA for oxidation reactions.

ACKNOWLEDGEMENTS

This research was supported by the Technology Innovation Program (10082572, Development of Low Energy Desalination Water Treatment Engineering Package System for Industrial Recycle Water Production) funded by the Ministry of Trade, Industry & Energy (MOTIE, Korea) and Korea Ministry of Environment as Global Top Project (Grant number: 2016002110008).

SUPPORTING INFORMATION

Additional information as noted in the text. This information is available via the Internet at http://www.springer.com/chemistry/journal/11814.

REFERENCES

1. J. Radjenovic and D. L. Sedlak, *Environ. Sci. Technol.*, **49**, 11292 (2015).
2. B. P. Chaplin, *Environ. Sci. Process. Impacts*, **16**, 1182 (2014).
3. J. Jeong, C. Kim and J. Yoon, *Water Res.*, **43**, 895 (2009).
4. G. Hurwitz, P. Pornwongthong, S. Mahendra and E. M. V. Hoek, *Chem. Eng. J.*, **240**, 235 (2014).
5. F. H. Oliveira, M. E. Osugi, F. M. M. Paschoal, D. Profeti, P. Olivi and M. V. B. Zanoni, *J. Appl. Electrochem.*, **37**, 583 (2007).
6. C. A. Martínez-Huitle and E. Brillas, *Angew. Chem. Int. Ed.*, **47**, 1998 (2008).
7. J. Kim, C. Kim, S. Kim and J. Yoon, *Korean Chem. Eng. Res.*, **53**, 531 (2015).
8. I. Sirés, E. Brillas, M. A. Oturan, M. A. Rodrigo and M. Panizza, *Environ. Sci. Pollut. Res.*, **21**, 8336 (2014).

9. S. Trasatti, *Electrochim. Acta*, **45**, 2377 (2000).
10. P. Roy, S. Berger and P. Schmuki, *Angew. Chem. Int. Ed.*, **50**, 2904 (2011).
11. G. K. Mor, O. K. Varghese, M. Paulose, K. Shankar and C. A. Grimes, *Sol. Energy Mater. Sol. Cells*, **90**, 2011 (2006).
12. B. D. Yao, Y. F. Chan, X. Y. Zhang, W. F. Zhang, Z. Y. Yang and N. Wang, *Appl. Phys. Lett.*, **82**, 281 (2003).
13. B. Chen, J. Hou and K. Lu, *Langmuir*, **29**, 5911 (2013).
14. D. Regonini, C. R. Bowen, A. Jaroenworaluck and R. Stevens, *Mater. Sci. Eng. R Reports*, **74**, 377 (2013).
15. J. M. Macak, B. G. Gong, M. Hueppe and P. Schmuki, *Adv. Mater.*, **19**, 3027 (2007).
16. Y. C. Nah, I. Paramasivam and P. Schmuki, *ChemPhysChem*, **11**, 2698 (2010).
17. R. P. Vitiello, J. M. Macak, A. Ghicov, H. Tsuchiya, L. F. P. Dick and P. Schmiki, *Electrochem. Commun.*, **8**, 544 (2006).
18. Y. L. Pang and A. Z. Abdullah, *Appl. Catal. B Environ.*, **129**, 473 (2013).
19. J. H. Park, S. Kim and A. J. Bard, *Nano Lett.*, **6**, 24 (2006).
20. X. Lu, G. Wang, T. Zhai, M. Yu, J. Gan, Y. Tong and Y. Li, *Nano Lett.*, **12**, 1690 (2012).
21. S. P. Hong, S. Kim, N. Kim, J. Yoon and C. Kim, *Korean J. Chem. Eng.*, **36**, 1753 (2019).
22. H. Wu, D. Li, X. Zhu, C. Yang, D. Liu and X. Chen, *Electrochim. Acta*, **116**, 129 (2014).
23. C. Kim, S. Kim, J. Choi, J. Lee, J. S. Knag, Y. Sung, J. Lee, W. Choi and J. Yoon, *Electrochim. Acta*, **141**, 113 (2014).
24. C. Kim, S. Kim, J. Lee, J. Kim and J. Yoon, *ACS Appl. Mater. Interfaces*, **7**, 7486 (2015).
25. C. Kim, S. Kim, S. P. Hong, J. Lee and J. Yoon, *Phys. Chem. Chem. Phys.*, **18**, 14370 (2016).
26. C. Kim, S. Lee, S. Kim and J. Yoon, *Electrochim. Acta*, **222**, 1578 (2016).
27. S. Kim, C. Kim, J. Lee, S. Kim, J. Lee, J. Kim and J. Yoon, *ACS Sustain. Chem. Eng.*, **6**, 1620 (2018).
28. J. Kim, C. Kim, S. Kim and J. Yoon, *J. Ind. Eng. Chem.*, **66**, 478 (2018).
29. A. Ahmadi and T. Wu, *Environ. Sci. Water Res. Technol.*, **3**, 534 (2017).
30. H. Zhou and Y. Zhang, *J. Power Sources*, **272**, 866 (2014).
31. J. Kim, C. Lee and J. Yoon, *Ind. Eng. Chem. Res.*, **57**, 11465 (2018).
32. A. Kapałka, G. Fóti and C. Comninellis, *Electrochem. Commun.*, **10**, 607 (2008).
33. Y. Jing and B. P. Chaplin, *Environ. Sci. Technol.*, **51**, 2355 (2017).
34. C. Barrera-Díaz, P. Cañizares, F. J. Fernández, R. Natividad and M. A. Rodrigo, *J. Mex. Chem. Soc.*, **58**, 256 (2014).